CROSS SECTIONS OF THE ^{56}Fe (n,α)^{53}Cr AND ^{54}Fe (n,α) ^{51}Cr REACTIONS IN THE MEV REGION

Yu.M. Gledenov[1], Guohui Zhang[2], M.V. Sedysheva[1], Zhimin Wang[2], G. Khuukhenkhuu[3], L.Krupa[4,5], Xiao Fan[2], Luyu Zhang[2], Huaiyong Bai[2], Jinxiang Chen[2]

[1]*Frank Laboratory of Neutron Physics, Joint Institute for Nuclear Research, Dubna 141980, Russia*
[2]*State Key Laboratory of Nuclear Physics and Technology, Institute of Heavy Ion Physics, Peking University, Beijing 100871, China*
[3]*Nuclear Research Centre, National University of Mongolia, Ulaanbaatar, Mongolia*
[4]*Flerov Laboratory of Nuclear Reactions, Joint Institute for Nuclear Research, Dubna 141980, Russia*
[5]*Institute of Experimental and Applied Physics, Czech Technical University in Prague, Horska 3a/22, Prague 2, 12800 Czech Republic*

Abstract

Natural iron and enriched ^{56}Fe and ^{54}Fe foil samples were prepared. Cross sections of the ^{56}Fe(n,α)^{53}Cr and ^{54}Fe(n,α)^{51} reactions were measured at E_n = 5.5, 6.5 MeV and E_n = 4.0, 4.5, 5.5 and 6.5 MeV, respectively, using a double-section gridded ionization chamber. A deuterium gas target was used to produce monoenergetic neutrons through the ^{2}H(d,n)^{3}He reaction. Two rounds of experiments were performed at the 4.5-MV Van de Graaff Accelerator of Peking University. Foreground and background were measured in separate runs. The neutron flux was monitored by a BF_3 long counter. The cross section of the ^{238}U(n,f) reaction was used as standard. Present results are compared with TALYS-1.6 code prediction, existing measurements and evaluations.

Introduction

Iron is one of the most important structural materials in nuclear science and engineering. For example, it is considered as one of the highest priority elements in the International Thermonuclear Experimental Reactor and International Fusion Material Irradiation Facility projects [1]. Recently, the CIELO Collaboration international cooperation also put the 56Fe isotope on the first priority list to clarify discrepancies among different nuclear data libraries of evaluations and measurements [2]. The cross-sectional data of charged particle emission reactions induced by neutrons are needed for evaluations of nuclear heating and radiation damage. Due to the (n,α) reaction, in particular, helium gas accumulated in the material causes serious embrittlement problems in reactors and other high-energy installations.

Cross sections of the ^{56}Fe(n,α)^{53}Cr and ^{54}Fe(n,α)^{51}Cr reactions were measured at E_n = 5.5 and 6.5 MeV and E_n = 4.0, 4.5, 5.5, and 6.5 MeV, respectively, using a double-section gridded ionization chamber as the α-particle detector. Natural iron and enriched ^{56}Fe and ^{54}Fe foil samples were prepared. A deuterium gas target was used to produce monoenergetic neutrons through the ^{2}H(d,n)^{3}He reaction. Two rounds of experiments were performed at the 4.5-MV Van de Graaff Accelerator of Peking University. Present results are compared with those of the TALYS-1.6 code calculations, existing measurements, and evaluations.

For the ^{56}Fe(n,α) ^{53}Cr reaction, only two measurements exist in the neutron energy range of 8–15 MeV [3,4], among which only one datum from Ref. [3] at E_n=8 MeV is included in the EXFOR library [5]. For the ^{54}Fe(n,α)^{51}Cr reaction only four measurements exist at neutron energies below 8 MeV, and there have been large differences as several times among them.

Since the (n,α) reaction channel for both ^{56}Fe and ^{54}Fe will open and increase rapidly in the MeV region, accurate cross-sectional data in this energy region are important. Although most of the evaluated nuclear data libraries contain these two reactions, there are large discrepancies among them, both in trend and in magnitude [6]. So, new and accurate measurements are needed to clarify these discrepancies.

Measurements and results

The experiments were performed for two rounds at the 4.5-MV Van de Graaff accelerator of Peking University, China. In the first round, the ^{56}Fe(n,α)^{53}Cr reaction was measured at E_n=6.5 MeV using the natural iron samples, and the ^{54}Fe(n,α) ^{51}Cr reaction was measured at E_n=5.5 and 6.5 MeV using the enriched ^{54}Fe samples. In the second round the ^{56}Fe(n,α) ^{53}Cr reaction was measured at E_n=5.5 and 6.5 MeV using enriched ^{56}Fe samples, and the ^{54}Fe(n,α)^{51}Cr reaction was measured at E_n= 4.0, 4.5, and 5.5 MeV using the same enriched ^{54}Fe samples as the first round. Measurements in the two rounds were repeated at 6.5 MeV for the ^{56}Fe(n,α)^{53}Cr reaction and at 5.5 MeV for the ^{54}Fe(n,α)^{51}Cr reaction to check the reliability of our experiments.

Neutrons were produced through the ^{2}H(d,n)^{3}He reaction by using a deuterium gas target. The α-particle detector is a double-section gridded ionization chamber (GIC) with a common cathode, and its structure can be found in Ref. [7]. The metal foil samples were prepared using the press.

Two-dimensional spectra of the cathode-anode coincidence signals for forward and backward directions were recorded separately from which the number of α events from the measured (n,α) reactions can be obtained.

Figures 1 and 2 show the results after background subtraction in which the counts between the 0◦ and the 90◦ curves represent the α events from the ^{56}Fe(n,α)^{53}Cr and ^{54}Fe(n,α)^{51}Cr reactions, respectively.

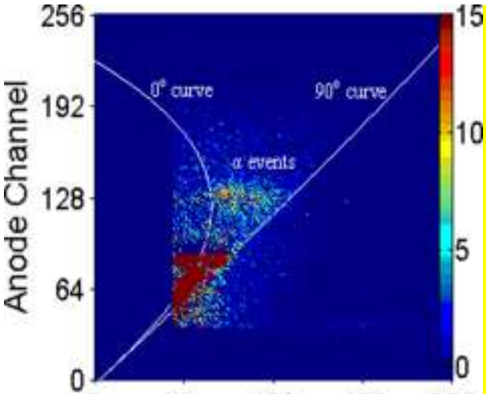

Fig. 1. Two-dimensional spectrum of the ^{56}Fe(n,α)^{53}Cr reaction at E_n=6.5 MeV (forward direction after background subtraction).

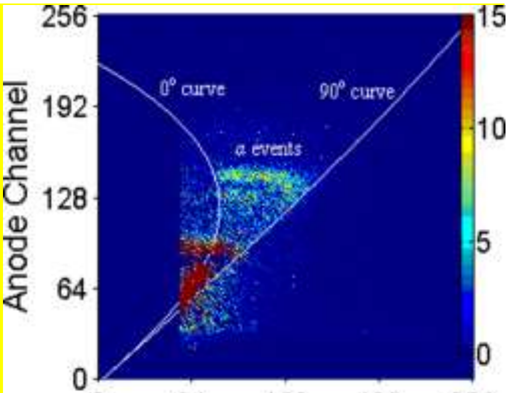

Fig. 2. Two-dimensional spectrum of the ^{54}Fe(n,α)^{51}Cr reaction at E_n=6.5 MeV (forward direction after background subtraction).

The α counts above the threshold can be obtained from the anode spectrum. Figures 3 and 4 show the anode spectra after the projection of events between the 0◦ and the 90◦ curves in Figs. 1 and 2.

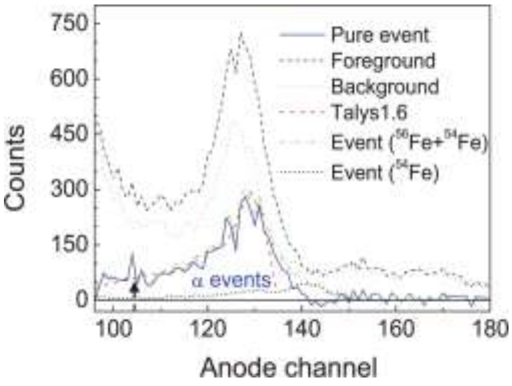

Fig. 3. Anode spectrum of the ^{56}Fe(n,α)^{53}Cr reaction at E_n = 6.5 (forward direction).

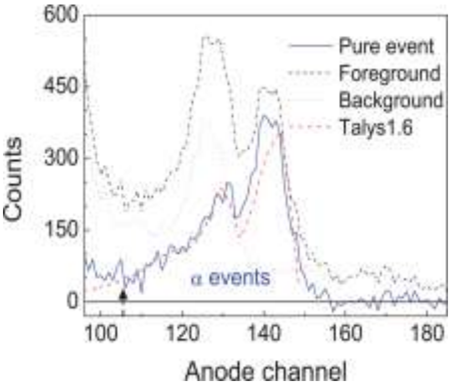

Fig. 4. Anode spectrum of the ^{54}Fe(n,α)^{51}Cr reaction at E_n = 6.5 MeV (forward direction).

Table 1. Measured and TALYS-1.6 calculated cross sections.

E_n (MeV)	^{56}Fe		^{54}Fe	
	σ_{exp} (mb)	σ_{TALYS} (mb)	σ_{exp} (mb)	σ_{TALYS} (mb)
4.0			0.76 ± 0.25b	0.18[d], 0.21[e]
4.5			0.36 ± 0.17b	0.54[d], 0.65[e]
5.5	1.05 ± 0.23[b]	0.59[d], 1.23[e]	3.21±0.38[a], 3.25± .43[b] 3.23 ± 0.29[c]	3.09[d], 3.80[e]
6.5	4.57 ± 0.52[a], 5.88 ± 0.79[b] 5.23 ± 0.47[c]	2.31[d], 4.62[e]	12.86 ± 1.13[a]	9.64[d], 13.37[e]

[a] Results measured in the first round of the experiment.

[b] Results measured in the second round of the experiment.

[c] Averaged over the first and second rounds of cross-sectional data.

[d] Predictions of TALYS-1.6 with default parameters.

[e] Predictions of TALYS-1.6 with adjusted parameters.

The measured results of the cross sections for the ^{56}Fe(n,α)^{53}Cr and ^{54}Fe(n,α)^{51}Cr reactions and calculation results using the TALYS-1.6 code with default and adjusted parameters are listed in Table 1. To fit the present results better, the factor of the potential depth parameter in the optical model ϑ_1 was adjusted from 1 (the default value) to 2 for the ^{56}Fe(n,α) ^{53}Cr reaction and from 1 (the default value) to 1.2 for the ^{54}Fe(n,α)^{51}Cr reaction. The adjustable range of the parameter ϑ_1 is from 0.1 to 10 [15].

The final results of the present paper are compared with those of existing measurements, evaluations, and TALYS-1.6 calculations as shown in Figs. 5 and 6.

Our measurements at 5.5 and 6.5 MeV support the data of the JENDL-4.0, JEFF-3.2, FENDLE-2.1, and CENDL-3.1 libraries in the MeV region. Further measurement for the ^{56}Fe(n,α) ^{53}Cr reaction at neutron energies higher than 7 MeV is necessary. For the ^{54}Fe(n,α)^{51}Cr reaction Our results agree with those of Meadows and Paulsen measured using the activation technique.

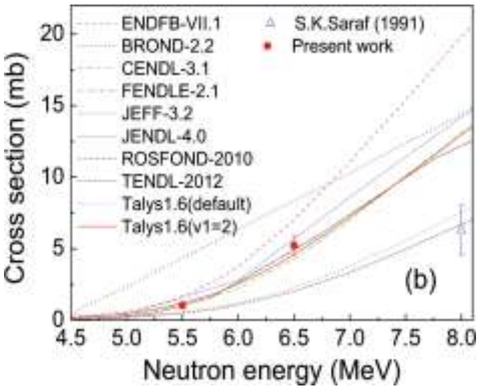

Fig. 5. Present cross sections of the ^{56}Fe(n,α)^{53}Cr reaction compared with existing measurements and evaluations for the neutron energy region from 4.5 to 8.0 MeV.

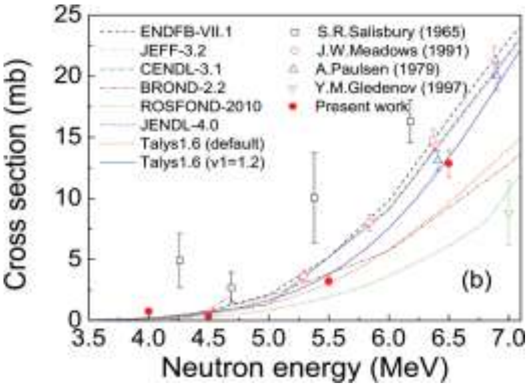

Fig. 6. Present cross sections of the ^{54}Fe(n,α) ^{51}Cr reaction compared with existing measurements and evaluations for the neutron energy region from 3.5 to 7.0 MeV

References

1. U. Fisher, P. Batistoni, E. Cheng, R. A. Forrest, and T. Nishitani, in Nuclear Data for Fusion Energy Technologies: Requests, Status and Development Needs, edited by R. C. Haight, M. B. Chadwick, T. Kawano, and P. Talou, AIP Conf. Proc. No. **769** (AIP, New York, 2005), p. 1478.
2. M. B. Chadwick, E. Dupont, E. Bauge, A. Blokhin et al., Nuclear Data Sheets **118**, 1(2014).
3. S. K. Saraf, C. E. Brient, P. M. Egun, S. M. Grimes, V. Mishra, and R. S. Pedroni, Nucl. Sci. Eng. **107**, 365 (1991).
4. S. M. Grimes, R. C. Haight, K. R. Alvar, H. H. Barschall, and R. R. Borchers, Phys. Rev. C **19**, 2127 (1979).
5. EXFOR: Experimental Nuclear Reaction Data, database version of January 7, 2015 [https://www-nds.iaea.org/exfor/exfor.htm].
6. ENDF: Evaluated Nuclear Data File, database version of October 22, 2014 [https://www-nds.iaea.org/exfor/endf.htm].
7. X. Zhang, Z. Chen, Y. Chen, J. Yuan, G. Tang, G. Zhang, J. Chen, Y. M. Gledenov, G. Khuukhenkhuu, and M. Sedysheva, Phys. Rev. C **61**, 054607 (2000).